

Stable finite difference discretizations of the forward speed seakeeping problem*

Harry B. Bingham,[†] Mostafa Amini Afshar, Robert Read, and Allan P. Engsig-Karup
 Mechanical Engineering, and Applied Math. & Computer Sci.
 Technical University of Denmark
 E-mail: hbb@dtu.dk, maaf@dtu.dk, rrea@dtu.dk apek@dtu.dk

This abstract presents a matrix-based stability analysis of high-order finite difference discretizations of the linearized seakeeping problem at non-zero forward speed. With forward speed, the critical stability properties of the solution are governed by the treatment of the convective terms in the free surface boundary conditions. A centered treatment of these terms is shown to be stable on a uniformly spaced horizontal grid, but an up-winded bias is required to achieve stability on non-uniformly spaced grids. Full up-winding of the terms is found to be unstable for schemes which employ more than three grid points on the stencil. Very strong grid stretching combined with high-order schemes can also lead to instability. A simple 2D example of the evolution of an initial free-surface pulse is also shown to verify that the analysis holds in practice.

We adopt a Cartesian coordinate system with the z -axis vertical and $\mathbf{x} = [x, y]$ the horizontal coordinates. The system is in steady translation along the x -axis with speed U . A potential flow solution in this moving frame is indicated by $\phi(\mathbf{x}, z, t)$. In the linearized, forward-speed seakeeping problem, we seek to evolve the free-surface elevation $\zeta(\mathbf{x}, t)$ and the velocity potential on the free-surface $\tilde{\phi} = \phi(\mathbf{x}, 0, t)$, using the free-surface boundary conditions which can be written

$$\partial_t \begin{bmatrix} \zeta \\ \tilde{\phi} \end{bmatrix} = \begin{bmatrix} U \partial_x & \partial_z \\ -g & U \partial_x \end{bmatrix} \begin{bmatrix} \zeta \\ \tilde{\phi} \end{bmatrix} \Rightarrow \partial_t \mathbf{f} = \begin{bmatrix} U \mathbf{D}_x & \mathbf{D}_n \\ -g \mathbf{I} & U \mathbf{D}_x \end{bmatrix} \mathbf{f}. \quad (1)$$

Here ∂_i indicates partial differentiation with respect to the variable i , and g is the gravitational acceleration. We focus here on the Neumann-Kelvin linearization of the problem for simplicity, but for other linearizations the convective terms will be modified to include the steady base flow solution. We adopt a method of lines solution and discretize the problem in space using arbitrary order finite difference schemes as described in detail by [7, 5, 1]. Thus we define a grid of N_x points on the free-surface with discrete solution values $\mathbf{f} = [\zeta_1; \zeta_2; \dots; \zeta_{N_x}; \tilde{\phi}_1; \tilde{\phi}_2; \dots; \tilde{\phi}_{N_x}] = [\mathbf{z}_0; \mathbf{p}_0]$, and replace the continuous differential operators by the rank N_x discrete matrix operators \mathbf{D}_x and \mathbf{D}_n to bring the continuous form on the left of (1) to the discrete form on the right. \mathbf{I} is the rank N_x identity matrix. The matrix \mathbf{D}_x takes the x -derivative of either ζ or $\tilde{\phi}$ at every grid point on the free-surface, while \mathbf{D}_n (the Dirichlet-to-Neumann operator) requires solving the Laplace problem in the entire fluid domain to get the surface vertical velocity from the surface potential at every surface grid point. When discretized as described in the above mentioned references, the continuous Laplace problem becomes the discrete linear system of equations

$$\mathbf{A} \mathbf{p} = \mathbf{b} \quad (2)$$

where \mathbf{A} is the rank $N = N_x N_z$ sparse matrix Laplacian operator including all boundary conditions, \mathbf{p} is a vector of discrete values of $\phi(\mathbf{x}, z)$ at all N grid points in the computational domain, and \mathbf{b} is a vector of zeros except where non-homogeneous boundary conditions are imposed. Generally, we solve this problem iteratively using a multigrid preconditioned defect correction

*The authors wish to thank the EU 7th Framework Programme (grant # 266030, ULYSSES) for funding, and the Danish Center for Scientific Computing for supercomputing resources.

[†]Presenting author

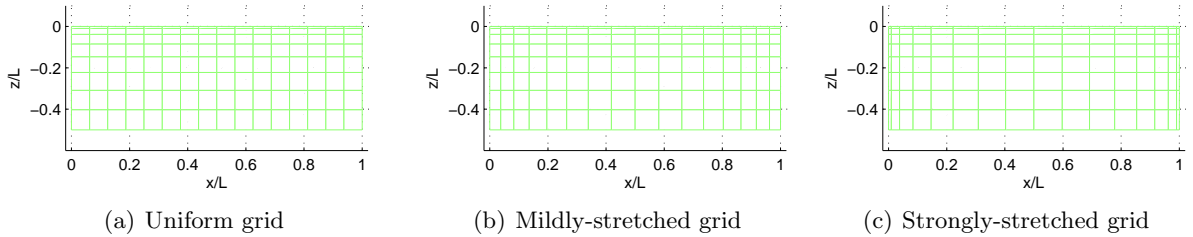


Figure 1: Representative grids with $N_x = 17$ & $N_z = 10$.

or GMRES method for maximum efficiency, but for the purposes of analysis on relatively small problems, we can explicitly build the \mathbf{D}_n matrix operator as

$$\mathbf{D}_n = \mathbf{D}_z^0 \mathbf{A}^{-1} \mathbf{P}^0 \quad (3)$$

where \mathbf{D}_z^0 is the N_x by N matrix which takes the vertical derivative of \mathbf{p} at each free surface grid point and \mathbf{P}^0 is the N by N_x matrix which holds the boundary condition information and gives $\mathbf{b} = \mathbf{P}^0 \mathbf{p}_0$.

The discrete Jacobian matrix of (1) is thus of rank $2N_x$, and we denote its eigenvalues by λ . The time-step size is Δt . Absolute stability for a given combination of time-integration method and spatial finite difference scheme is ensured only when all the values of $\Delta t \lambda$ lie within the stability region of the time-stepping method. This is a standard matrix-based stability analysis and has been applied to this method of solving the zero-speed problem by [5, 1], and to solving the forward-speed problem using Rankine-type Boundary Element Methods (BEMs) by [3]. In [4] the technique was also applied to a Mixed Eulerian-Lagrangian (MEL) solver at zero-speed. A number of authors have carried out a spectral Von-Neumann stability analysis of BEM solutions to the problem *e.g.* [2, 6, 8]. The advantage of the matrix-based approach is that non-uniformity in the grid, internal structures and non-periodic boundary conditions can all be taken into account; which is important for getting a true picture of the behavior of a method in practice. Due to the required inversion of a large matrix however, the analysis is limited to relatively small problems.

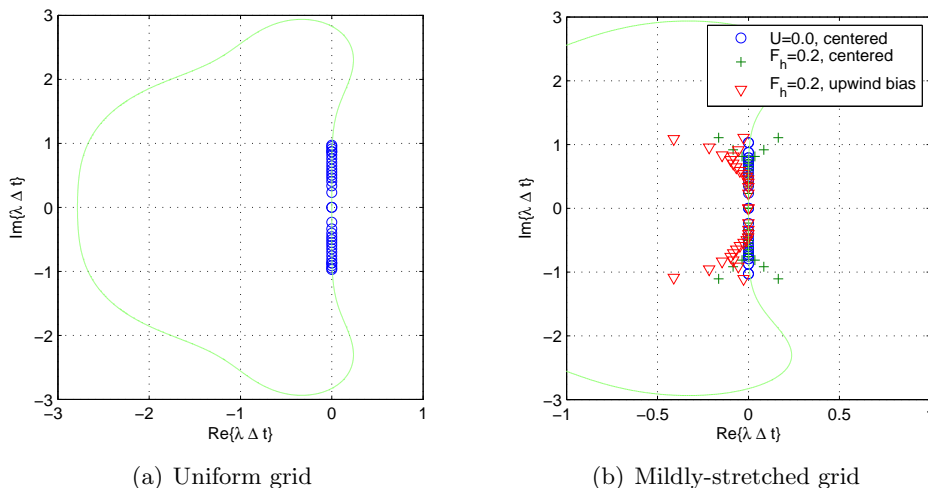


Figure 2: (a): Stability eigenvalues for a uniform grid with $N_x = 17$, $N_z = 10$, $r = 7$, $F_h = 0.2$, $C_r = 1$; also showing the stability region for RK44 time-stepping. (b): Stability eigenvalues for the mildly-stretched grid at zero and non-zero speed using centered and upwind-biased discretizations of the convective terms.

We consider a 2D rectangular domain of length L and water depth h , discretized as shown in Fig. 1 using $N_x = 17$ and $N_z = 10$ grid points (including a “ghost point” below the bottom which

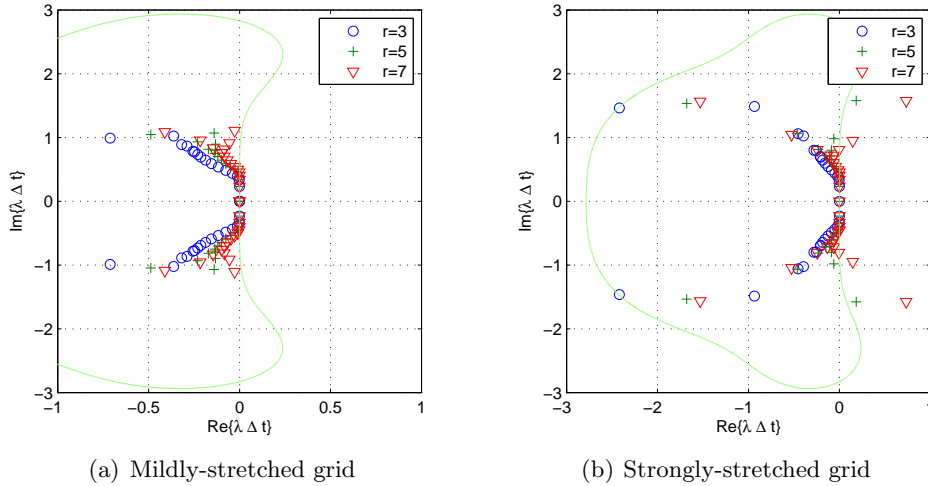


Figure 3: (a): Stability eigenvalues for a mildly stretched grid using upwind-biased differencing for convection and different stencil sizes r . (b): Stability eigenvalues for a strongly-stretched grid under the same conditions.

is not shown but is used to satisfy the bottom boundary condition). A cosine stretching in the vertical is used for both grids to improve the resolution near the free-surface. The left-hand grid has a uniform spacing in the horizontal while the right-hand grid uses a mild-stretching towards the boundaries based on the mapping $\xi = \tanh(Cs)/\tanh C$ where s is a uniform grid and C is a constant controlling the stretching which in this case is set to 1.0.

Fig. 2(a) plots the stability eigenvalues on the uniform grid using $r = 7$ -point (6th-order) centered finite difference schemes for a forward speed corresponding to a grid Froude number $F_h = U/\sqrt{g\Delta x} = 0.2$ and a Courant number $C_r = (U + \sqrt{Lg/2\pi})\Delta t/\Delta x = 1.0$. Also shown here is the stability region for the explicit fourth-order, four-stage Runge-Kutta method which we use for time-stepping. From this plot we can see that the solution is well behaved with pure imaginary eigenvalues running from -1 to 1 indicating a neutrally stable solution with no diffusion. In Fig. 2(b) we plot the eigenvalues on the mildly stretched grid for three conditions. The blue circles show the result at $U = 0$ and they lie nicely along the imaginary axis indicating that the stretched grid is also well behaved in this case. The green crosses show the result using a centered scheme at $F_h = 0.2$ and we can see that some eigenvalues have moved off the axis indicating diffusion when they are inside the stability region and instability when they lie outside the stability region. Eigenvalues with positive real part will remain outside the stability region no matter how small we make Δt , so this scheme is clearly unconditionally unstable. When centered schemes are used, and the grid spacing decreases in the direction of the flow, downstream points receive a stronger weighting than upstream points which leads to a classical down-winding situation and hence instability. To avoid this, we introduce a one-point, upwind-bias in the \mathbf{D}_x operator by shifting the finite difference stencil one point in the upstream direction. The red triangles in this plot show the result for this upwind-biased scheme which can be seen to stabilize the method.

Fig. 3(a) shows how the eigenvalues of the upwind-biased scheme behave on the mildly-stretched grid for stencil sizes of $r = 3, 5$ & 7 ; while plot (b) shows the same result but on a strongly-stretched grid where a cosine spacing has been applied towards both boundaries. Here we can see that while the 3-point scheme remains stable in this case, the higher-order schemes produce unstable eigenvalues. Though not shown here, increasing the upwind-shift of the higher-order schemes does not lead to stable methods.

To verify that this analysis holds in practice, we have run a simple 2D example of the evolution of an initial free-surface disturbance given by $\zeta(x, 0) = -2(x - x_0)e^{-\frac{(x-x_0)^2}{2\sigma}}$ with $x_0 = 20L$ and $\sigma = 0.3L^2$, on a domain of length $40L$, depth $h = 5L$, moving at a Froude number of

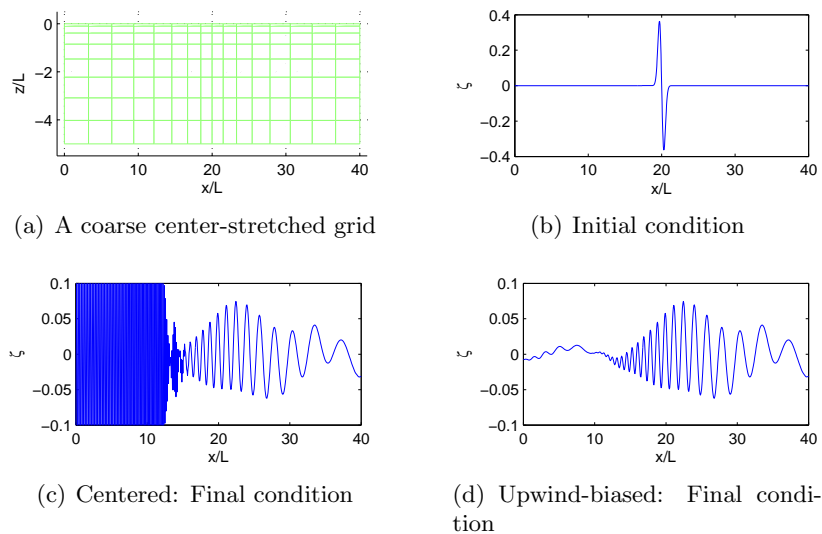


Figure 4: Evolution of an initial free-surface disturbance with $F = U/\sqrt{gL} = 0.2$.

$F = U/\sqrt{gL} = 0.2$. This is meant to mimic a scattered wave from a ship of length L located at the center of the domain and thus the grid is clustered towards the center. The pulse is resolved by about 50 grid points with a total of $N_x = 481$; with $N_z = 10$, $r = 7$ and $C_r = 1$. The boundary conditions at the ends of the computational domain are fully reflecting, and implemented by reflecting all finite difference coefficients for a symmetric function. Fig. 4 shows a very coarse image of the grid, the initial condition and a snapshot of the surface elevation after the ship has travelled around twelve ship lengths, using both centered and upwind-biased convection. Clearly the centered method is unstable while with upwind-biasing the results show no signs of instability no matter how long the calculations continue.

References

- [1] H. B. Bingham and H. Zhang. On the accuracy of finite difference solutions for nonlinear water waves. *J. Engineering Math.*, 58:211–228, 2007.
- [2] B. Büchmann. Accuracy and stability of a set of free-surface time-domain boundary element models based on B-splines. *Int. J. Num. Methods in Fluids*, pages 125–155, 2000.
- [3] B. Büchmann. Theory and applications in stability of free-surface time-domain boundary element models. *Int. J. Num. Methods in Fluids*, pages 321–339, 2001.
- [4] G. Colicchio and M. Landrini. On the use of boundary-integral equation methods for unsteady free-surface flows. *J. Engineering Math.*, 46:127–146, 2003.
- [5] A. P. Engsig-Karup, H. B. Bingham, and O. Lindberg. An efficient flexible-order model for 3D nonlinear water waves. *J. Comput. Phys.*, 228:2100–2118, 2009.
- [6] D. C. Kring. *Time domain ship motions by a three-dimensional Rankine panel method*. PhD thesis, Massachusetts Institute of Technology, Cambridge, Massachusetts, 1994.
- [7] R. Read and H. B. Bingham. An overset grid approach to linear wave-structure interaction. In *31st Intl. Conf. on Offshore Mech. and Arctic Eng.*, Rio di Janiero, Brazil, 2012.
- [8] T. Vada and D. E. Nakos. Time-marching schemes for ship motion simulations. In *8th Intl. Wrkshp. Water Waves and Floating Bodies*, St. John’s, Newfoundland, 1993. <http://www.iwwwfb.org>.